



# Predicted ecological consequences of wave energy extraction and climate-related changes in wave exposure on rocky shore communities

Andrew Want <sup>1,2,\*</sup>, Simon Waldman<sup>2,3</sup>, Michael T. Burrows<sup>4</sup>, Jonathan C. Side<sup>1</sup>, Vengatesan Venugopal<sup>3</sup>, Michael C. Bell<sup>1</sup>

<sup>1</sup>International Centre for Island Technology, Heriot Watt University, Stromness, Orkney KW16 3AN, United Kingdom

<sup>2</sup>Energy and Environment Institute, University of Hull, Hull HU6 7RX, United Kingdom

<sup>3</sup>Institute for Energy Systems, School of Engineering, University of Edinburgh, Edinburgh EH9 3DW, United Kingdom

<sup>4</sup>Scottish Association for Marine Science, Scottish Marine Institute, Oban PA37 1QA, United Kingdom

\*Corresponding author. Energy and Environment Institute, University of Hull, Hull HU6 7RX, United Kingdom. [a.want@hull.ac.uk](mailto:a.want@hull.ac.uk)

## Abstract

Wave energy has the potential to contribute in the transition to decarbonized electricity generation. Extracting wave energy might be expected to have ecological impacts on rocky shore intertidal communities where exposure is one of the most important factors determining species structure and composition. With global climatic change, coastal exposure is predicted to increase with greater significant wave height. The wave-exposed west coast of Orkney, Scotland, UK, is the site of pre-commercial wave device testing. Surveys of 39 rocky shore sites along this coast identified key species and abundances, and quantified exposure-modifying topographic variables. A spectral wave model was constructed to compare baseline, wave extraction, climate change, and combined scenarios. Generalized additive modelling was used to describe the relationship between species, topography, and exposure. Results show that individual species differentially respond to exposure changes with 'winners' and 'losers' at site level. Overall, community responses are expected to be far greater following predicted climatic change than to industrial-scale wave energy extraction, depending on spatial scale. In combination, energy extraction may reduce the effects of climate-change-related increases in wave exposure of rocky shores. Predicting how location-specific biotic assemblages respond to changes in wave energy as a result of long-term forcing agents provides a valuable marine resource management tool.

**Keywords:** rocky shore; renewable energy; exposure; climate change; topography; littoral

## Introduction

Wave energy has the potential to make significant contributions to decarbonization of electricity generation in the UK (Neill et al. 2017, Greaves et al. 2020, Jin and Greaves 2021), with an aspiration for 22 GW of installed capacity by 2050 (Wave Energy Road Map 2020 for the UK). Evidence on environmental impacts of wave energy developments is required if this target is to be achieved. This paper addresses the potential impacts of a reduction of wave energy on intertidal organisms on highly exposed shores likely to be downstream of wave energy developments.

Given the nascent state of the industry, it is not surprising that there is a paucity of studies using direct measurements to address the environmental and ecological consequences of wave energy developments (Frid et al. 2012, Langhamer 2016). Inferences on some types of impact may be drawn from studies of offshore wind farms (e.g. Wilhelmsson and Malm 2008, Lindeboom et al. 2011); this might include physical impacts of development on the seabed (Shields et al. 2011), collision risks and behavioural disturbance to marine mammals, fish, and birds (Wilson et al. 2006, Waggitt et al. 2016), noise pollution (Farcas et al. 2016), and more [see Copping and Hemery (2020) for a full review]. 'Downstream' effects from deployment of wave energy converters (WECs), particu-

larly in large-scale farms, would be expected to stem from changes in wave climate, principally by reducing energy levels reaching the shoreline or interacting with the surrounding benthic community (Lohse et al. 2008, Shields et al. 2011). Effects are most likely to be manifested in the littoral zone, where hydrodynamic forces from wave exposure are greatest (Denny 1995, Gaylord 2000). Wave interactions with the boundary layer and the benthos will increase in the nearshore as depth decreases (Shields et al. 2011), creating a potentially important locus for responses to wave energy extraction on the rocky shoreline.

Wave energy is one of the most important factors determining the structure and composition of biological communities on rocky shores (Denny 1995). This is typically manifest as differences in abundances and vertical distribution of organisms correlated with energy exposure (Ballantine 1961, Lewis 1964). Even slight changes in exposure may result in shifts in species distribution and morphology (Crothers 1985, Ruuskanen and Nappu 2005, Wolcott 2007, Blanchette et al. 2008). Remarkably little is known, however, of the specific facets of exposure that form this relationship (Thomas 1986, Denny 1999, Gaylord 2000, Burel et al. 2022). Closer examination of exposure reveals a complex interaction of elements, including fetch (Burrows et al. 2008), local and distant

meteorological conditions (Sundblad *et al.* 2014), nearshore bathymetry (Folley and Whittaker 2009), and shore topography (Thomas 1986). Topographic modifiers of waves approaching and breaking on the shore may include slope, orientation relative to the predominant wave direction, and structural complexity (Smith 2003, Burrows *et al.* 2008, Folley and Whittaker 2009, Sundblad *et al.* 2014). In order to develop an understanding of the potential ecological responses to changes in wave climate, we must thus consider both incoming wave energy and dissipation of this energy by nearshore and littoral features.

The relationship of hard substrate community composition to wave exposure is well known and recognized as a fundamental distinction in marine habitat classification (Connor *et al.* 2004). This is not to say, however, that we can expect the ecological response to a reduction of wave energy by WECs to be a simple transition between biotopes at different locations on an axis of wave exposure. Given the nature of the wave resource, WECs would be expected to be located ‘upstream’ of highly exposed shores, and that such shores would likely remain at the upper end of the exposure gradient even after the reduction of wave energy. Understanding of the ecological response to energy extraction thus depends on characterizing relationships of species abundance *within* a subset of highly exposed shores, rather than between exposed and sheltered shores.

Climate change is a crucial context for considering potential impacts of wave energy extraction. This is firstly because climate-driven changes in marine ecosystems and range shifts in marine biota are already apparent, and this is particularly evident in littoral environments (Parmesan and Yohe 2003, Burrows *et al.* 2011). These observed changes may be due largely to increasing sea temperature, but climate models also predict associated increases in frequency and intensity of storm conditions (Collins *et al.* 2013, Woolf and Wolf 2013). Irrespective of the proximate drivers of background change, ecological monitoring must account for this shifting baseline before it is possible to detect and characterize responses to wave energy extraction. The context of climate change is also important for predictive studies, not just because the extraction of wave energy is itself intended to reduce greenhouse gas emissions, but because it may also have the potential to ameliorate the effects of increased storminess on wave heights at a local scale. Setting aside effects of increased temperatures, in this study, we predict responses of intertidal communities to changes in wave exposure related to climate change and wave energy extraction, separately and combined.

The rocky shores of West Mainland Orkney (WMO) provide an ideal case study for addressing such effects in an area identified as highly suitable for wave energy developments (Scottish Government 2016). This coast is extremely exposed; nearshore significant wave height is frequently >5 m and maximum wave period is frequently >20 s (EMEC 2022). Predominant wind and wave direction is from the west meaning that the westerly orientated cliffs are facing the dominant direction of fetch. Spatial contrasts in wave energy received at the shore are determined by nearshore bathymetry, and mediated by shore topography. Since the WMO coast is geologically uniform and encompassed within a modest extent of ~25 km north–south, it may be assumed that environmental drivers of variation in intertidal communities are local in scale (dom-

inated by wave exposure and shore topography) without confounding effects of biogeography and larger-scale environmental variation. Comprehensive biological survey data are available for the entire stretch of this coast from a study by Want (2017), providing a unique resource for characterizing intertidal communities at the upper end of the wave exposure gradient. The area is also within the domain of a numerical wave model constructed as part of the EcoWatt 2050 project, which includes projections for large-scale wave developments with and without concurrent climate change (EcoWatt 2050 2017).

The aims of this paper are (1) to characterize the relationship between abundance of intertidal biota and wave energy *within* a subset of high-energy sites in a location relevant to wave energy developments; (2) to use this characterization to predict the changes in abundance likely to result from modification of the wave climate by the presence of WECs operating in adjacent waters; and (3) to identify the separate roles of energy extraction and climate change in determining changes in abundance. The overarching research question is, would we expect a detectable biological response to wave energy extraction?

## Methods

### Rocky shore surveys

Rocky shores were accessed at 39 sites on WMO (Fig. 1). The survey area included rocky shores located within, and distant from, leasing sites for large-scale deployment of WECs (Marine Scotland 2022). All sites were accessed at low water of spring tides in early summer during 2013–2015 (Want 2017). Surveys focussed on stable rock surfaces rather than mobile substrates such as boulder fields or coarse sediments in embayments. Sites were defined as discrete rock units of 10–20 m in length, taking the form of a rock platform, stretch of cliff base or an emerged reef. Access by rigid-hulled inflatable boat was required for 19 sites. All sites were surveyed by the same surveyor (AW) during an approximate 45-min period.

The abundance of rocky shore species was assessed at each site using the semi-quantitative SACFOR scale, as described by Crisp and Southward (1958) and modified by Hiscock (1981). Abundance was scored as S = superabundant, A = abundant, C = common, F = frequent, O = occasional, R = rare, or N = absent. Thresholds for these determinations depend on the natural abundance scales of the different species at small spatial scales (Appendix 1). SACFOR scores were determined for 45 species selected to cover trophic levels represented by typical rocky shore organisms, ranging from primary producers to secondary consumers (Appendix 2). All species were evaluated on open rock surfaces where they are fully subject to exposure, rather than in the lee of rock features or in crevices where abundance of certain species may be higher (e.g. blue mussel, *Mytilus edulis*).

Two indices of shore topography were recorded at each survey site. Shore slope was defined as the angle to which the rock surface is inclined to the horizontal plane, parallel to the direction of dip. This was determined using a digital protractor at three positions considered to be characteristic of each site. Substrate complexity was scored on a 10-point semi-quantitative scale to assess the presence or absence of rock features that would be expected to mediate the interaction between waves and the substrates on which the

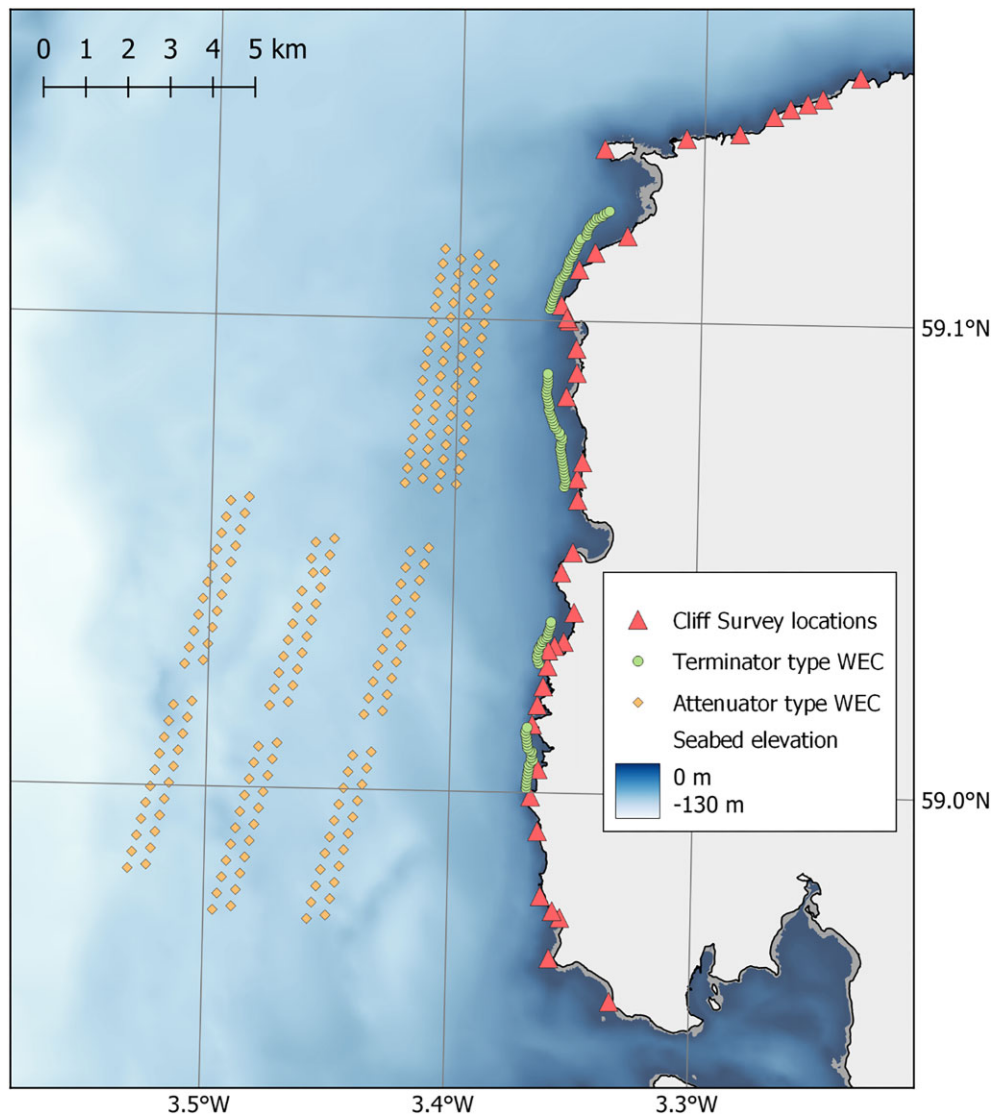


**Figure 1.** Bathymetric map of rocky shore survey sites along WMO. Placement of terminator and attenuator type wave energy converting devices as part of a proposed energy extraction scenario are indicated.

**Table 1.** Substrate complexity: semi-quantitatively scored on a scale from 1 to 10 applied to rocky shore surveys based on the presence and absence of rock features, which might be expected to complicate the interaction between wave energy and the substrate, including broken shores, rock pools, steps, and offshore rocks or skerries.

Score	Description of features
1	Uncomplicated platform featuring minimal deviation from ‘planar’ surface
2–4	Minimal presence of low, stepped features, small and shallow rock pools, and little or no offshore rock features
5–6	Increasingly broken shores with larger steps, deeper and more numerous rock pools, and presence of small offshore rock features
7–9	Broken shores with combinations of gullies, varied rock pools, substrates providing distinct seaward and leeward surfaces, and large offshore rocks or skerries
10	Unusually contorted shore with all features present in maximal level of complexity, and presence of several offshore rock features

Within score ranges described later, e.g. 2–4, sites are scored dependent on how much features are shared within the category and with categories above and below. Representative images of rocky shore complexity scores are provided in [Appendix 3](#).

organisms were recorded ([Table 1](#); [Appendix 3](#)). Given limited time available for access to shore sites, this scale was developed as a practicable alternative to established direct and indirect methods for quantifying topographic complexity

([Frost et al. 2005](#), [Wilding et al. 2010](#)). Topographic assessment at each site was completed prior to SACFOR surveys, to avoid biases owing to preconceived associations between species’ abundance and shore exposure.

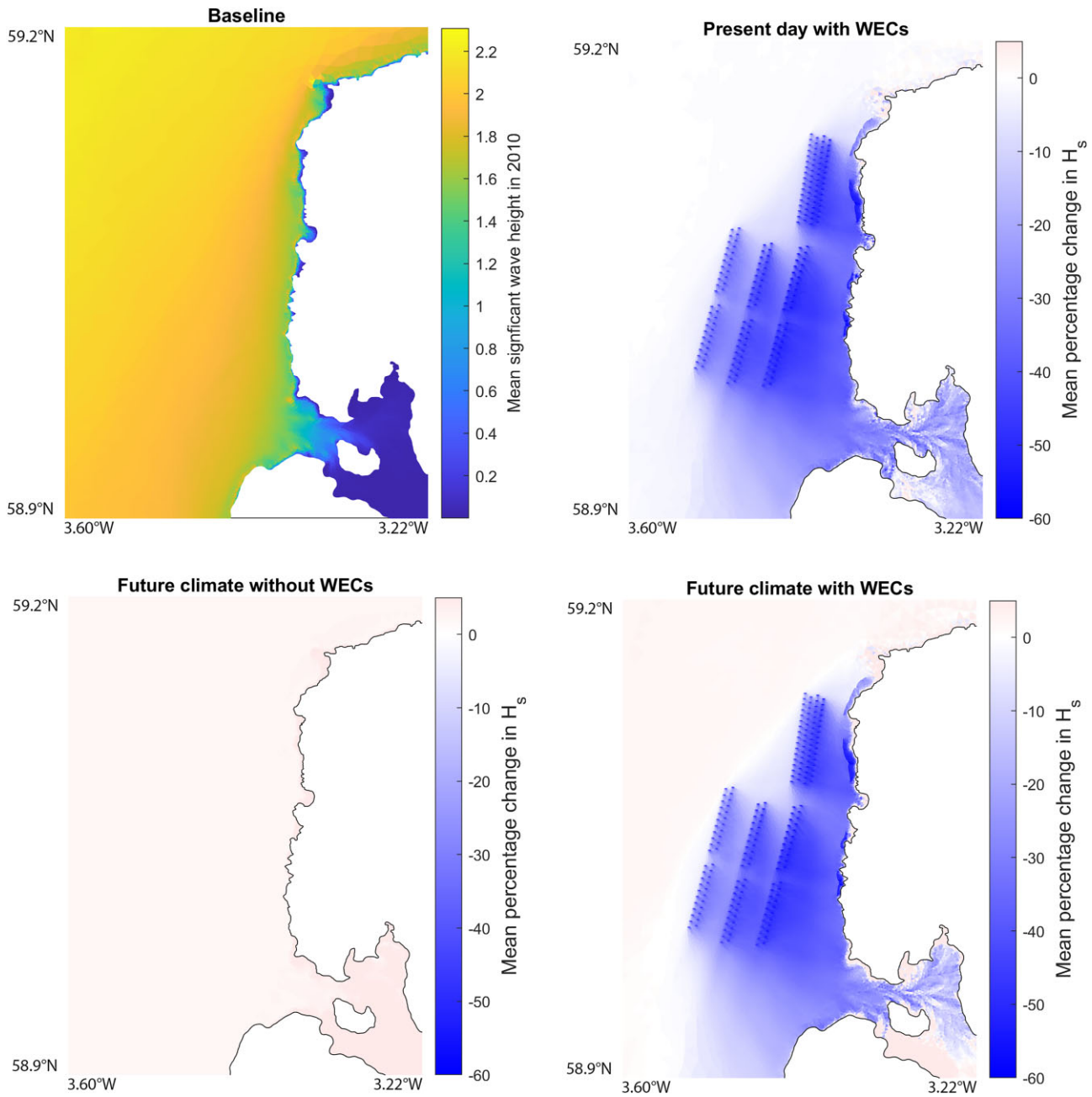


**Figure 2.** Four scenarios of present day and future wave climates on WMO, based on spectral wave modelling. Baseline: mean significant wave height ( $H_s$ ) in 2010; present day with WECs: predicted mean percentage change in  $H_s$  in 2010; future climate without WECs: predicted mean percentage change in  $H_s$  in 2050; future climate with WECs: predicted mean percentage change in  $H_s$  in 2050.

### Numerical wave model and projection scenarios

A spectral wave model (DHI 2022) covering the WMO region was constructed and used to simulate four scenarios: baseline (recent: 2010), with recent (2010) energy extraction (EE), with future (2050) climate change (CC), and with future (2050) energy extraction and climate change (EE + CC) (Fig. 2).

The model used an unstructured triangular mesh with a typical resolution of 150–200 m in the baseline version. The scenarios with energy extraction had a higher resolution around the WECs. This regional wave model was forced by a larger-scale model of the North Atlantic, which was in turn driven by wind data sourced from the European Centre for Medium-range Weather Forecasts (ECMWF 2018). Wave parameters

were output at a 30-min temporal resolution. For a detailed description of the baseline spectral wave models, see Venugopal and Nimalidinne (2015) and Venugopal et al. (2017).

Two types of WECs were simulated: a line attenuator type [similar to the Pelamis P2 design by Pelamis Wave Power (Yemm et al. 2012)] and a surge-based terminator type [similar to the Oyster 800 design by Aquamarine Power (Cameron et al. 2010)]. A wave-structure interaction modelling tool (WAMIT 2022) was used to simulate small groups of devices at a high resolution and predict the wave transmission, reflection, and absorption coefficients that should be used to describe their behaviour in the regional-scale spectral model. In reality these parameters would depend on the sea state, but in

**Table 2.** Rocky shore taxa selected for modelling of abundance in relation to exposure, with frequency of SACFOR scores across 39 shore sites on WMO.

Taxon	Phylum	Frequency of SACFOR scores						Not observed
		S	A	C	F	O	R	
<i>Porphyra umbilicalis</i>	Rhodophyta	6	11	15	4	0	0	3
<i>Palmaria palmata</i>		8	8	6	2	4	0	11
<i>Corallina officinalis</i>		8	13	16	1	1	0	0
<i>Mastocarpus stellatus</i>		1	12	14	7	3	0	2
Red turf*		8	13	12	2	4	0	0
<i>Cladophora rupestris</i>	Chlorophyta	6	2	6	0	1	0	24
<i>Ulva intestinalis</i>		3	8	12	5	2	0	9
<i>Scytosiphon lomentaria</i>	Ochrophyta	0	1	7	9	8	3	11
<i>Alaria esculenta</i>		26	7	1	0	1	1	3
<i>Fucus distichus anceps</i>		6	12	6	2	2	2	9
<i>Fucus serratus</i>		0	3	0	1	2	0	33
<i>Fucus spiralis nanus</i>		1	7	5	2	2	0	22
<i>Fucus vesiculosus linearis</i>		2	7	1	1	0	0	28
<i>Himantalia elongata</i>		4	6	5	2	0	2	20
<i>Actinia equina</i>	Cnidaria	0	4	5	1	5	2	22
<i>Patella vulgata</i>	Mollusca	0	0	12	6	8	0	13
<i>Patella ulyssiponensis</i>		0	11	15	3	7	0	3
<i>Nucella lapillus</i>		0	3	2	0	1	2	31
<i>Mytilus edulis</i>		0	4	10	14	9	0	2

\*Abundance of small rhodophytes forming a turf at mid to low shore level, predominantly *Callithamnion* spp., *Ceramium* spp. (including *Ceramium shuttleworthianum*), and *Polysiphonia broidieii*.

order to simulate the greatest energy extraction, and hence the ‘worst case’ in terms of environmental impact, the values used were those for the sea state in which the WECs would produce their maximum output. For further details of this process the interested reader is referred to Venugopal et al. (2017) and Tay and Venugopal (2017).

WECs with a total generating capacity of ~245 MW were included in the energy extraction scenarios, comprising 198 attenuators in offshore locations (depths of 40–80 m, 3–10 km from the coast) and 120 terminators in inshore waters (depths of 10–20 m, 300–1000 m from the coast), within The Crown Estate’s designated lease zones for wave energy development off WMO (The Crown Estate 2015) (Fig. 2). Array layouts were based on scoping reports for proposed wave energy developments, as described by O’Hara Murray and Gallego (2017).

The baseline and EE simulations were run for the year 2010. This is considered representative of the wave climate at the time of the shore surveys (2013–2015).

Future wave scenarios (CC and CC + EE) were based on predictions for the year 2050. Due to the stochastic nature of wave energy, simply running the wave models with predictions of winds in 2050 would have left ambiguity over whether any differences from the present day were due to climate change, or due to random variations between the two years in question. Instead, the approach adopted was to take the forcing data for 2010 and scale it in line with expected changes in significant wave heights. Scaling was based on a global ocean model produced by the EU RISES-AM project (Bricheno and Wolf 2018). Data on significant wave heights were analysed for a 30-year baseline period centred on 1985 and a 30-year future period centred on 2050 based upon the IPCC RCP8.5 climate pathway (Riahi et al. 2011). Percentile-based scaling factors were applied to re-map data to the projected future distribution. In addition, sea level rise was simulated by

applying a datum correction of 25 cm to the model bathymetry, based on the predicted global mean sea level rise for 2050 under RCP8.5 (IPCC 2014).

### Statistical modelling of species abundance

Generalized additive models (GAMs) were used to describe the relationship of species’ abundance with wave exposure and topographic variables, using the mgcv package in R (Wood 2017, R Core Team 2018). SACFOR scores were treated as ordered categories on a seven-point scale (0 = absent, 1 = Rare, through to 6 = Superabundant), considering abundance as a logistically distributed latent (unobserved) variable to be modelled as a function of environmental predictors. Model selection was undertaken using the ‘select = TRUE’ option of the mgcv gam procedure, which allows terms to be removed by being penalized to zero (Wood 2017). Both main effects and first-order interactions were specified using tensor product smooth terms, and the Restricted Maximum Likelihood method was used for parameter estimation.

The value for the latent variable, estimated through the linear predictor for the model, is compared with cut points that determine the predicted category (SACFOR score) for an observation (Wood et al. 2016, Wood 2017). Given a vector of cut points  $\theta$  for categories  $j$  and a linear predictor value  $\lambda_j$  for a set of predictor variables  $j$ , the cumulative probabilities for ordered categories  $i = 1$  to  $I - 1$  are calculated using the inverse logistic function:

$$c_{ij} = \frac{1}{1 + e^{-(\theta_i - \lambda_j)}}$$

By definition, the cumulative probability for the last category,  $c_{Ij}$ , is 1. Probabilities of each score level are then easily calculated as differences in cumulative probabilities. Given the small sample size (39 sites), the full range of SACFOR scores

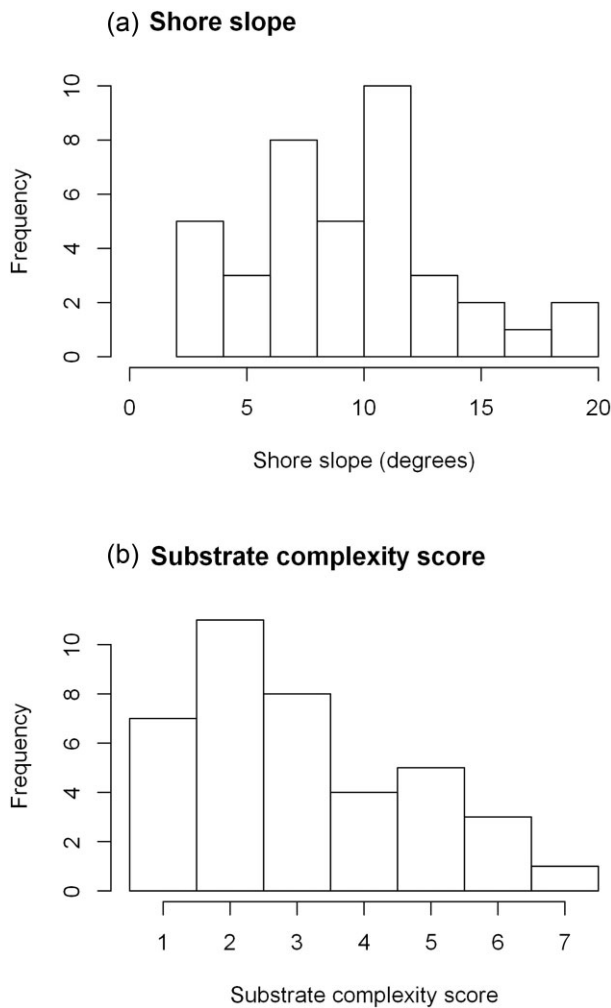


**Figure 3.** Distributions of slope and substrate complexity values for shore survey sites in WMO. Refer to text and Table 1 for explanation of these topographic measures.

was not observed for every taxon, so the number of cut points for the latent variable was adjusted accordingly, and the probabilities of the unobserved scores were set to zero. Fitted values from the GAM models were re-scaled to SACFOR scores by using the probabilities of category membership as weights in calculating weighted means of the values (0 to 6) assigned to the SACFOR levels.

### Treatment of environmental variables

Three environmental variables were included in the GAM fitting. Firstly, significant wave height ( $H_s$ ) was selected to represent incoming wave energy, based on monthly mean values extracted from the wave model outputs (see above). The resolution of the unstructured grid was 100–150 m close to the shore. Littoral survey locations were adjacent to, but outside, the margins of the model grid domain, hence model outputs are not available at the exact survey locations. Extrapolation beyond the model domain would likely be spurious, hence a strategy was needed to represent the wave climate in the immediate vicinity of the survey sites. Nearest neighbour values were considered but appeared unduly sensitive to variability at the grid margin, hence an averaging strategy was used based on water depth and distance from the survey sites. After

screening of various options, monthly averages of cell outputs were calculated for each site selected by a maximum distance of 50 m and a maximum depth of 9 m. This ensured that the values represented the vicinity of the survey sites, inshore of the modelled locations of wave energy extraction. Screening indicated that the GAM modelling was not sensitive to the exact choice of distance and depth values, nor to the choice of month. January was selected as representative of typical extreme winter conditions. During this period, wave damage from seasonal storms is at its most critical as an ecological factor, although wave action during periods of larval or spore attachment can be more important (Vadas et al. 1990).

Secondly, shore complexity and shore slope were selected to represent aspects of the shore that would modify the exposure of littoral organisms to incoming wave energy. Shore complexity was considered because it would be expected that dissipation of hydrodynamic energy caused by interaction of the incoming wave with the shore surface would increase with topographic complexity (Smith 2003, Lowe et al. 2007). Note that, while structural complexity would be expected to increase the availability of shelter at small spatial scales (Johnson et al. 1998), restriction of SACFOR determination to open rock surfaces (see above) means that this component of modified exposure is not relevant for the survey data. Shore slope was considered because the dynamics of breaking and slamming forces associated with incoming wave movements would be expected to be strongly related to slope (Peregrine 1983, Smith 2003), in ways that would not be captured by the bathymetry of the wave model domain. Shore slope was represented in the GAM models by the average of the three measurements made at each site. Other environmental variables recorded for the survey sites by Want (2017), such as wave fetch values and shore aspect, were not included in the GAM models, as these are considered as proxies for incoming wave energy accounted for by modelled  $H_s$  values.

Projections of the wave model for EE, CC, and EE + CC scenarios used  $H_s$  values processed in the same way as those from the baseline model. Site-specific shore complexity and slope values remained unchanged in the model projections.

### Model inference on response of species abundance to changes in wave climate

Whilst the smooth terms estimated in the GAM models are of interest in showing the nature of responses to exposure and topographic variables, it is of more interest to explore overall model inferences over ranges of current environmental conditions and scenarios of change. This approach is also better suited for exploring the influence of interaction terms in the models, and for quantifying the risks/probabilities of specific responses occurring.

Exploratory analyses were undertaken using bootstrap sampling of the data set coupled with model averaging based on Akaike weights (Burnham and Anderson 2002). However, the final approach used was posterior inference, as described by Wood (2017), based on the penalized fitting procedure described above. This involved mapping of model coefficients to fitted curves to obtain linear predictors for ranges of environmental variables, simulation of coefficient vectors from their posterior distribution (multivariate normal) and application of these vectors to the linear predictor matrix to obtain model predictions for each replicate. We applied the posterior simulation approach with 10 000 replicates. Model

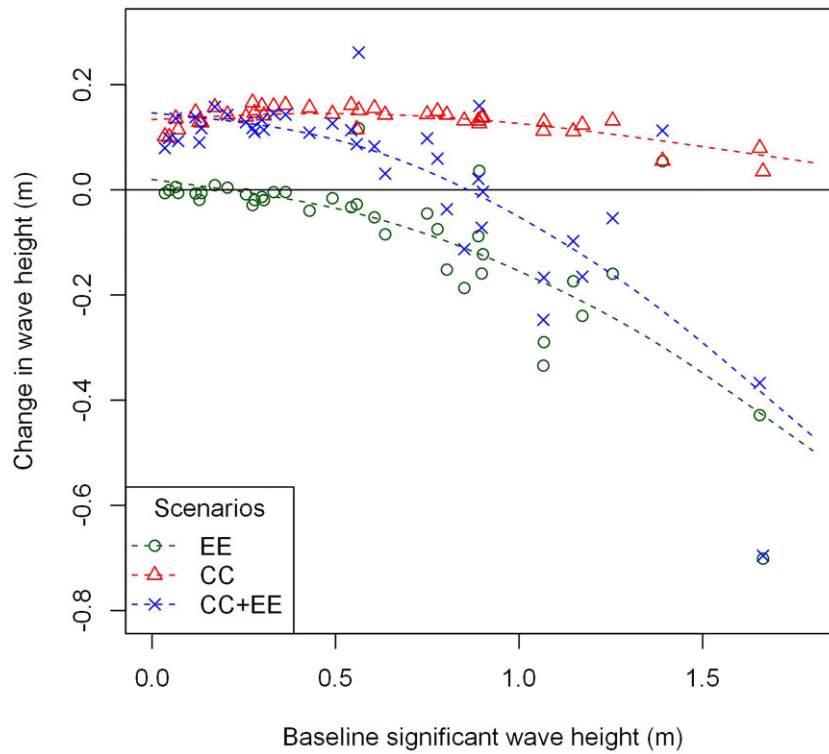


**Figure 4.** Changes in significant wave height applying to shore survey sites on WMO for scenarios of wave EE, CC, and the two combined (CC + EE). Dashed lines are fitted smoothing splines for the relationship between change and baseline values.

predictions were then re-scaled to SACFOR scores, as described above.

As noted by Wood (2017), posterior simulation is preferable to bootstrapping, partly because the latter is more expensive in processing time, but also because the appearance of data more than once in a bootstrap set leads to under-smoothing. For our small dataset ( $n = 39$ ), bootstrapping was also problematic because of lack of contrast in response variables in some samples. Allowing terms to be penalized to zero in fitting the model was also more efficient than averaging over the hierarchy of models with different combinations of environmental variables, although this is at the expense of some loss of efficiency in specifying main effects separately from interaction terms.

### Metrics of ecological response

Model predictions and posterior inference were used to explore model behaviour and the sensitivity of species' responses to ranges of environmental variables. The same approach was used to evaluate effects of changed wave conditions using projections of the wave model under scenarios of EE, CC, and a combination of the two (CC + EE) (see above). Distributions of response metrics across posterior simulation replicates were summarized by percentiles at 2.5%, 50%, and 97.5%, estimated using the default method for the R quantile function, providing measures of central tendency, and 95% confidence intervals.

Model behaviour was summarized by SACFOR-scaled responses to the observed range of significant wave heights,  $H_s$ . To capture the effects of first-order interactions between the environmental variables, these responses were represented for

low, mid, and high values of shore slope and complexity, based on their observed ranges.

Three metrics were used to summarize the responses of each species to the scenarios of change. Firstly, for each scenario, we considered the risk of observing an 'important' change in abundance. An operational definition of an ecologically important change in rocky shore species abundance in response to environmental change could be characterized as one that is detectable by survey, i.e. an average SACFOR score changing by one unit or more. The risk can thus be calculated in terms of the proportion of posterior simulation replicates for which baseline and projected SACFOR values differ by one or more units:

$$R^s = \frac{\sum_{i=1}^I \sum_{j=1}^J r_{ij}^s}{I \times J},$$

where  $R^s$  is the risk for scenario  $s$ ,  $I$  is the number of posterior simulation replicates and  $J$  is the number of sites.  $r_{ij}^s$  takes the value of 1 if  $|P_{ij}^s - B_{ij}| \geq 1$ , where  $P_{ij}^s$  is the projected SACFOR score for replicate  $i$  and site  $j$  under the conditions of scenario  $s$ , and  $B_{ij}$  is the baseline fitted SACFOR score for replicate  $i$  and site  $j$  under current conditions, otherwise is zero. This is easily modified to calculate the risk of changes in a positive or negative direction.

Secondly, directional change in abundance was calculated for each posterior simulation replicate:

$$D_i^s = \frac{\sum_{j=1}^J (P_{ij}^s - B_{ij})}{J},$$

where  $D_i^s$  is the change metric for replicate  $i$  in scenario  $s$ .

Thirdly, the magnitude of shift in abundance was calculated as:

$$S_i^s = \frac{\sum_{j=1}^J |P_{ij}^s - B_{ij}|}{J},$$

where  $S_i^s$  is the shift metric for replicate  $i$  in scenario  $s$ . The change and shift metrics are calculated as averages across sites, representing responses at the scale of the overall study area. The distributions of  $D_i^s$  and  $S_i^s$  across replicates were summarized by percentiles, as above.

## Results

### Species abundance and environmental data

Nineteen taxa were recorded sufficiently frequently across the 39 survey sites, and with sufficient contrast in abundance levels to merit further analysis (Table 2). These comprised 14 algae and 5 animal taxa. *Alaria esculenta* was the most abundant taxon, being recorded as ‘Superabundant’ at two thirds of survey sites.

Shore slope ranged from 2.2° to 19.0° relative to the horizontal, with an average value of 9.3° (± 0.68° SE) (Fig. 3a). Complexity scores (Table 1) ranged from 1 (surface close to planar) to 7 (broken, with rock features), with the distribution skewed towards the lower (least complex) end of this range (Fig. 3b). Slope and complexity were uncorrelated (Spearman’s rank correlation  $r_s = -0.012$ ,  $df = 37$ ,  $P = 0.943$ ).

Mean January significant wave heights ( $H_s$ ) varied between sites from 0.035 to 1.7 m, with an overall mean of 0.62 m (± 0.072 m SE) and values skewed towards the lower end of this range (Fig. 4). The distribution of values was shifted slightly downwards by energy extraction (scenario EE), substantially upwards by climate change (scenario CC), and slightly upwards when the effects of climate change were moderated by energy extraction (scenario CC + EE). The amount of change under each scenario varied between sites, those with the highest baseline  $H_s$  values tending to show the largest decreases (EE and CC + EE) or smallest increases (scenario CC). Average site-specific changes were: EE, -0.085 m; CC, +0.13 m; CC + EE, +0.030 m.

### GAM outcomes

Significant wave height and shore topography accounted for up to 52% of the deviance in the SACFOR scores for each of the 19 taxa considered (Table 3). The estimated degrees of freedom in Table 3 indicate the complexity of the smooth terms: zero represents a term weighted out of the model, a value close to 1 indicates an approximately linear term, higher numbers represent more complex curves. According to the approximate chi-square tests for the model terms reported by the mgcv gam procedure, terms including  $H_s$  were significant at  $P < 0.05$  for 16 out of 19 taxa considered, and at  $P < 0.1$  for all (Table 4). In twelve taxa, the effects of  $H_s$  were significantly modified through interaction with shore topography, while for the remaining seven  $H_s$  was primarily a main effect.

Model projections based on posterior simulation are illustrated for three example taxa in Appendix 4, focussing on the SACFOR response to  $H_s$ . The effects of interactive model terms are illustrated through plots at low, mid, and high levels of shore slope and complexity, based on the ranges of values present in the data set (slope 2°, 9°, and 19°; complexity

**Table 3.** Summary of ordered category GAM models fitted to SACFOR survey data for rocky shore taxa at 39 sites on WMO.

Taxon	$H_s$	Slope	Complex	$H_s \times \text{Slope}$	$H_s \times \text{Complex}$	Slope $\times$ Complex	% Deviance explained
<i>Porphyra umbilicalis</i>	0.0	0.0	0.2	4.6***	1.3**	0.0	23.6
<i>Palmaria palmata</i>	0.0	0.8*	0.0	0.8+	0.0	0.0	6.4
<i>Corallina officinalis</i>	1.0*	0.0	1.3*	0.5	1.4***	0.2	24.2
<i>Mastocarpus stellatus</i>	0.0	1.8***	1.4***	0.9***	0.0	4.9***	51.1
Red turf	0.3	0.8*	0.0	0.8	0.8*	3.5**	23.9
<i>Cladophora rupestris</i>	1.4**	0.6+	0.9*	0.0	2.8***	0.0	31.0
<i>Ulva intestimalis</i>	1.8*	0.0	1.0*	5.8***	1.2+	0.5	37.0
<i>Scytosiphon lomentaria</i>	0.9**	2.9***	1.3**	0.0	0.0	5.6***	51.6
<i>Alaria esculenta</i>	2.2***	1.4*	0.0	0.5	0.0	1.5**	39.3
<i>Fucus distichus anceps</i>	1.2**	1.8**	0.6	0.0	0.0	0.5	17.1
<i>Fucus serratus</i>	0.9**	1.5	0.0	0.0	0.0	1.4*	51.8
<i>Fucus spiralis nanus</i>	0.8*	0.6	0.0	2.6*	0.0	0.0	14.7
<i>Fucus vesiculosus linearis</i>	2.0*	0.1	0.0	0.9+	0.0	0.7	32.7
<i>Himantalia elongata</i>	2.3*	1.1***	0.8*	0.0	0.0	0.0	43.2
<i>Actinia equina</i>	1.1*	1.3*	1.5**	0.0	0.0	0.7	21.9
<i>Patella vulgata</i>	0.8*	0.0	0.8*	0.4	2.7+	0.6	31.6
<i>Patella ubyssiponensis</i>	0.8**	0.7	0.8+	5.0***	0.9***	0.0	36.1
<i>Nucella lapillus</i>	0.9*	1.7*	0.0	0.0	0.0	1.3*	31.4
<i>Mytilus edulis</i>	0.0	1.3**	0.8*	0.0	1.5***	0.7	21.7

Columns show the estimated degrees of freedom and the approximate significance (chi-square test) of each smooth term.  $H_s$  is significant wave height; Slope is the average angle of the rock platform with respect to the horizontal plane; complex indexes topographic complexity (see Table 1). Significance: \*\*\* $P < 0.001$ ; \*\* $P < 0.01$ ; \* $P < 0.05$ ; + $P < 0.1$ .

**Table 4.** Summary of contributions of significant wave height ( $H_s$ ) to the GAM models for abundance of rock shore taxa on WMO.

Taxon	$H_s$ main effect only	$H_s$ modified by shore slope	$H_s$ modified by shore complexity
<i>Porphyra umbilicalis</i>		×	×
<i>Palmaria palmata</i>		(×)	
<i>Corallina officinalis</i>			×
<i>Mastocarpus stellatus</i>		×	
Red turf		×	
<i>Cladophora rupestris</i>			×
<i>Ulva intestinalis</i>		×	(×)
<i>Scytosiphon lomentaria</i>	×		
<i>Alaria esculenta</i>	×		
<i>Fucus distichus anceps</i>	×		
<i>Fucus serratus</i>	×		
<i>Fucus spiralis nanus</i>		×	
<i>Fucus vesiculosus linearis</i>		(×)	
<i>Himantalia elongata</i>	×		
<i>Actinia equina</i>	×		
<i>Patella vulgata</i>			(×)
<i>Patella ulysiponensis</i>		×	×
<i>Nucella lapillus</i>	×		
<i>Mytilus edulis</i>			×

Significance of  $H_s$  as a main effect is indicated only for models in which interactions with shore slope or complexity were not significant at  $P < 0.1$  or better. ×, term significant at  $P < 0.05$  or better; (×), term significant at  $P < 0.1$ .

score 1, 3, and 7). SACFOR for *A. esculenta* is projected to be high over a wide range of  $H_s$  values but shows declines at very low values for some combinations of slope and complexity (Appendix 4–D1). *Fucus distichus anceps* shows a more straightforward relationship, with highest SACFOR scores projected for intermediate levels of  $H_s$ , with shore topography contributing minor scaling of the curve (Appendix 4–D2). In contrast, projections for *Patella ulysiponensis* indicate a much more complex interaction with shore topography (Appendix 4–D3). In this case, highest SACFOR values are generally projected for high values of  $H_s$ , but with very variable effects at lower values of  $H_s$ .

### Projections for scenarios of energy extraction and climate change

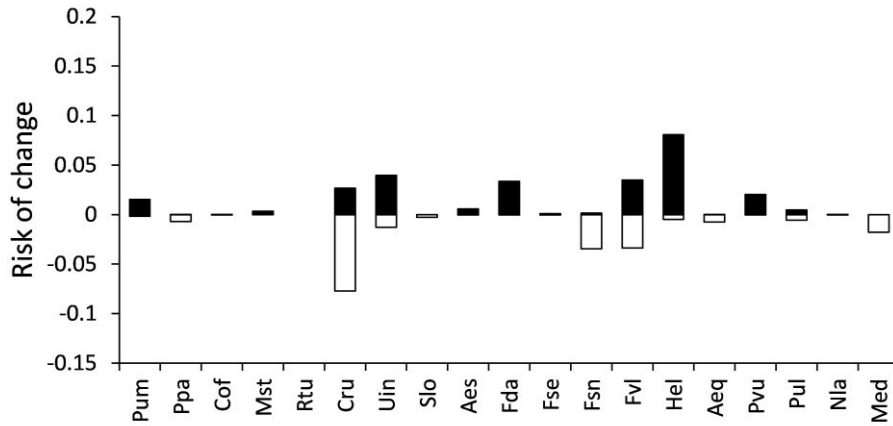
Risks of an ecologically ‘important’ response to the changes in  $H_s$  for each scenario are illustrated in Fig. 5. Positive and negative changes are distinguished by filled and open bars, respectively, and the combined length of the bar indicates the overall risk. In general, the risk of a change by one SACFOR unit or more appears low (<5%) for most taxa under Scenario EE, much higher under Scenario CC, and only slightly moderated from this level under Scenario CC + EE. The moderating effect of energy extraction on the response to climate change only is seen mostly at the higher levels of response. For example, in *Fucus vesiculosus linearis* the overall risk of an important response is reduced from 28% (CC) to 22% (CC + EE), similar scales of change applying to the positive and negative directional components of this risk. Other responsive taxa such as *Himantalia elongata* are somewhat similar, although in this case the response to energy extraction is predominantly positive. Examination of the distribution of responses between survey sites (not shown) indicates that the existence of both positive and negative risk for the responsive taxa is due to variation between sites rather than uncertainty about the nature of the response, i.e. there are ‘winners’ and ‘losers’ across the WMO coastline, depending on the spatial distribution of changes in wave climate.

Projected responses to energy extraction and climate change are further characterized by ordination diagrams showing average shifts and changes in SAFCOR for each scenario (Fig. 6). ‘Shift’ represents the overall responsiveness of taxa across sites, whereas ‘change’ represents the directional component (see the ‘Methods’ section). In most cases, as shown by 95% confidence bounds overlapping with the baseline, a directional component to the response is not apparent when considered across all survey sites, further indicating that both losses and gains would be expected with the overall change in wave climate. Again, responses to CC are much greater than to EE, and the former is not much moderated by the latter (CC + EE), except at more wave exposed sites (Fig. 4). Note, however, the scaling of the axes in Fig. 6, indicating that the scale of projected response is not dramatic. This is consistent with the view of ecologically important risk presented in Fig. 5. Note also that whilst the two ecological response metrics, ‘shift’ and ‘change’, may appear similar, they are of value in separating responses that are largely directional across all sites, typifying the animal taxa (bottom row in Fig. 6), from those where gains and losses balance out across the set of sites, exemplified by Rhodophyta and Chlorophyta taxa (top row in Fig. 6).

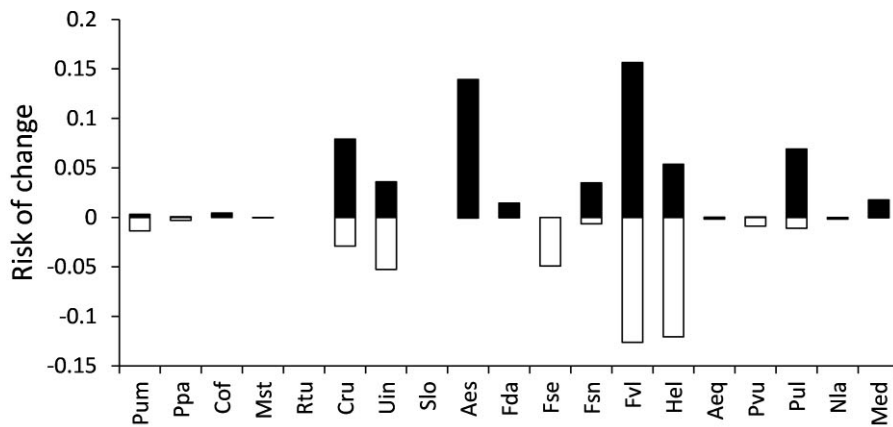
### Discussion

Rocky shore survey data and wave modelling outputs for WMO have provided a unique opportunity to assess the likely nature and scale of ecological response to extraction of wave energy. The location is in an area where WECs are being tested, and where commercial-scale deployment of these devices may occur in the future (Marine Scotland 2022). The results of our study show that even among sites that would all be classed as highly exposed, distinctions in the exact level of exposure are ecologically meaningful in determining the presence and abundance of rocky shore species. Between-site heterogeneity of effective exposure is indicated as being due to two sources, namely variations in incoming wave energy and onshore topography. First, nearshore bathymetry and

## (a) Scenario EE



## (b) Scenario CC



## (c) Scenario CC+EE

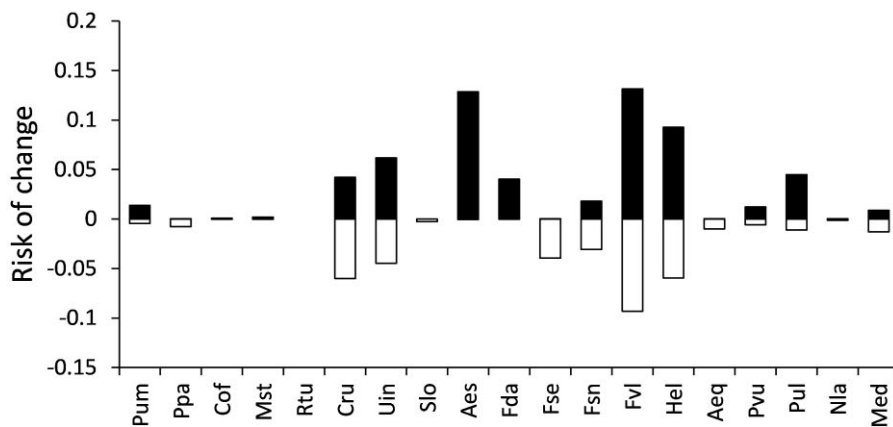


**Figure 5.** Projected responses of species abundance to changes in significant wave height under scenarios for (a) energy extraction (EE), (b) climate change (CC), and (c) climate change and energy extraction combined (CC + EE). Responses are characterized as risk of change in SACFOR score of one unit or more in either direction, measured across 10 000 posterior simulations of the GAM model and across all 39 survey sites. Taxon codes: Pum, *Porphyra umbilicalis*; Ppa, *Palmaria palmata*; Cof, *Corallina officinalis*; Mst, *Mastocarpus stellatus*; Rtu, red turf; Cru, *Cladophora rupestris*; Uin, *Ulva intestinalis*; Slo, *Scytosiphon lomentaria*; Aes, *Alaria esculenta*; Fda, *Fucus distichus anceps*; Fse, *Fucus serratus*; Fsn, *Fucus spiralis nanus*; Fvl, *Fucus vesiculosus linearis*; Hel, *Himanthalia elongata*; Aeq, *Actinia equina*; Pvu, *Patella vulgata*; Pul, *Patella ulyssiponensis*; Nla, *Nucella lapillus*; Med, *Mytilus edulis*.

coastline aspect, in our study accounted for within the wave model, determine wave climate approaching the littoral environment, causing substantial variation in average wave height between sites. Second, our results also highlight the impor-

tance of shore topography in determining effective local exposure to incoming wave energy, as represented by the abundance of characteristic species. The potential for ecologically important responses to changes in wave climate thus needs to

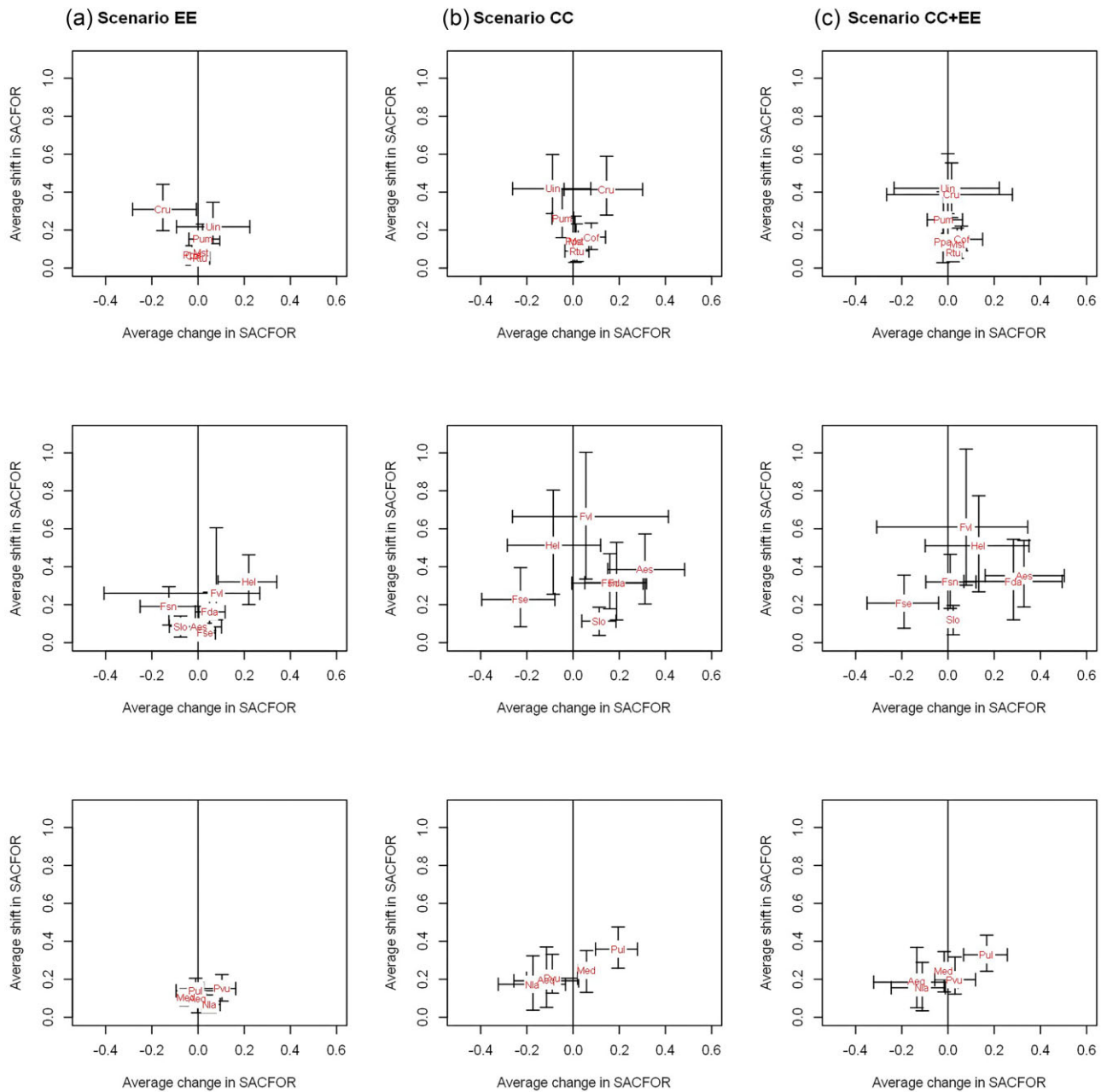


**Figure 6.** Ordination of species projected species response to scenarios of (a) energy extraction, (b) climate change and (c) climate change combined with energy extraction. “Shift” represents the overall responsiveness of taxa across sites, whereas “change” represents the directional component (see Methods). Taxon codes (see Fig. 5 legend) are located at the median of change and shift in SACFOR score across 10 000 posterior simulations of the GAM model, averaged across all sites. Vertical and horizontal bars represent 95% confidence intervals (2.5 and 97.5 percentiles of the distribution of simulated values) for shift and change statistics, respectively. For clarity, the plots are separated into Rhodophyta and Chlorophyta (top row), Ochrophyta (middle row) and animals (bottom row).

be considered at a local scale, taking account of topographical modifiers of exposure, here represented in terms of the structural complexity and slope of the shore.

The wave modelling outputs used here include projections for scenarios of commercial-scale energy extraction and climate change, allowing corresponding projection of the ecological response. At higher levels of exposure, energy extraction is expected to cause substantial decreases in wave height, irrespective of climate change with more sheltered sites predicted to remain relatively unaffected. Energy extraction is expected to decrease the scale of ecological responses to climate driven

changes in significant wave heights, at least in locations in the immediate lee of WECs. At a broader scale, the effects of climate change on significant wave heights are predicted to outweigh energy extraction as a driver of ecological change, with the latter expected slightly to decrease the scale of response to the former.

The wave energy extraction modelled in the current studies is based on plausible commercial-scale deployments of line attenuator and surge-based terminator technologies. However, because the energy absorption of WECs can be highly frequency-dependant and does not necessarily vary linearly

with incoming wave power, the actual effects on shorelines will depend on the specific WEC design and the specific wave conditions in a more complex way than is modelled here. For example, some WECs are designed to minimize their energy absorption during storms to avoid damage (Coe et al. 2018). These devices would attenuate everyday waves while allowing the highest energy storms to reach the shoreline almost unaffected, and so increase the difference in shoreline wave action between reduced energy in summer and unaffected high energy in winter. This could have consequences for species with highly seasonal patterns of growth where life processes during less energetic seasons are critical for persistence (Want et al. 2014). For species whose presence and abundance are primarily driven by acute, extreme events, extraction of wave energy during only more moderate conditions may have little direct consequence. Furthermore, although small changes in fetch have been shown to produce morphological changes in fucoids (Ruuskanen et al. 1999), and, similarly, such consequences might be expected from wave extraction, it is not correct to assume that WEC deployment results in a permanently limited or constrained level of exposure (analogous to fetch reduction) for the duration of a development's presence.

In the current study, January was selected as typifying winter conditions, when it is assumed that wave exposure is most critical as an ecological factor for many rocky shore species. WaveRider buoys deployed by the European Marine Energy Centre to monitor the wave resource at Billia Croo, WMO have recorded  $H_{\max}$  in winter storms of up to 19 m (EMEC 2022). While the current studies have not modelled extreme waves during storm events, it has been shown that in extreme events, over 10% of annual wave energy can arrive offshore in a storm lasting <24 h (Folley and Whittaker 2009). However, how changes in storm events might affect the community is not well understood (Thomas 1986, Blanchette et al. 2008) but may depend upon whether species are more responsive to changes in average, long-term wave exposure or to acute, extreme storm events (Siddon and Witman 2003, Ruuskanen and Nappu 2005, Wolcott 2007). While beyond the boundaries of the current study, companion work focused on seasonal differences in wave exposure impacts using this wave model would be welcomed.

Because of the small number of sites used in the analysis, it is inevitable that overfitting should be a concern in the GAM outputs. This is particularly the case given the inclusion of interaction terms in the model, which are necessary to account for the possible modification of received wave climate by shore topography. To some extent, overfitting is at least reduced by the model selection procedure applied, which should weight the contribution of each model term according to the evidence in the data to support it. However, it is undoubtedly true that a larger data set would provide a more robust basis for inference. Thus, for example, the complexity of the projected response of the limpet *Patella ulyssiponensis* to changes in wave energy under different combinations of shore complexity and slope (Appendix 4–D3) does not bear close interpretation, whilst at the same time this model output still represents the best inference given the available evidence. The constraint here—and the novelty—is that we are restricting the analysis to compare within a set of difficult-to-access high-exposure sites within a small region. This has the strength that the sites are representative of those likely to be affected by extraction of wave energy, and for which changes in wave climate have been modelled, whilst minimizing contrasts in biogeography, water

temperature and geology. Evidence on littoral species' response to wave energy extraction would certainly be improved, and generalised, by extension of shore surveys, wave modelling and analysis for other regions.

Another caveat for this modelling concerns the validity of the absolute  $H_s$  immediately adjacent to the shore given that bathymetric data are not available at these shallow depths. We assume, however, that the relative scaling of  $H_s$  values between sites is valid. This assumption would benefit from validation in future studies. At present, the available wave data are the best source of evidence on wave climate adjacent to these high energy shores.

The current study has identified several organisms, including key structuring species representing different trophic levels, which appear to be particularly sensitive to changes in exposure at the extreme high-end of this hydrodynamic gradient. These species may serve as valuable indicators of community responses to changes in wave exposure, especially on highly energetic, rocky shores. The magnitude of responses varies between species and between individual locations; there may be considerable variability in both magnitude and direction of change. The long-term, forcing agents of energy extraction and climate change are expected to produce 'winners' and 'losers' both at regional population scale and at localized individual sites.

The posterior simulation modelling approach used here has allowed the development of a risk-based framework for assessing the significance of the ecological response. Assessment of 'significance' depends, of course, on a set of criteria for acceptable limits of change, e.g. set by environmental managers or regulators. Such criteria do not exist, nor is there an objective basis for determining the consequences of changes for ecosystem structure and function or population viability. Nevertheless, it is clear that the risks of change detectable by SACFOR-based surveys (such as the MarClim programme, Mieszkowska et al. 2006) is highly variable between both sites and species, where a single category change represents an order of magnitude change. Studies by Burel et al. (2022) suggest that a wave height threshold may exist in the littoral zone above which rocky shore communities are dominated by barnacles and limpets, rather than fucoid macroalgae, the latter dominating less exposed shores. Our study did not show evidence of this threshold, possibly owing to the focus on the upper end of the wave energy gradient and the presence of extreme exposure adapted fucoids in the north of Scotland. Here (e.g. in Fig. 5), we focus on between-species differences. Considering the combined risk across all 39 sites, our analysis indicates that some Ochrophyta characteristic of high-energy shores, such as *Fucus vesiculosus linearis* and *Himantalia elongata* are likely to show both losses and gains at individual sites under the climate-change scenario, whereas other high-energy Ochrophyta, such as *Alaria esculenta* and *Fucus distichus anceps*, are more likely to show gains. These changes are slightly moderated by the addition of energy extraction to the climate scenario, and interestingly this applies to both gains and losses, presumably owing to site-specific factors.

Expected responses of a subset of species on WMO reveal that local topography does, at times, play a complicated role in ecological responses to changing exposure. The association of the high-exposure specialist kelp, *Alaria esculenta*, on steeply sloped and uncomplicated substrates is consistent with the greater abundances of this species on wave exposed shores. *Fucus distichus anceps*, a high-exposure ecotype fucoid, is

associated with steeply sloped, uncomplicated rocky platforms (Powell 1963, Munda 2004, Want 2017). There appears to be seemingly small interplay between these variables in the current studies. The complex interaction between community members which may be responding differentially to changes in exposure requires careful interpretation.

A simple monotonic relationship does not always exist between slope and high-exposure organisms, and a more complex relationship between these factors is observed in *P. ulysiponensis*. This may owe, in part, to the multifaceted role of slope on rocky shores including through mediation of water drainage, affecting desiccation stress (Benedetti-Cecchi et al. 2000). While more tolerant of greater exposure, *P. ulysiponensis* is more sensitive to desiccation than its congener, *P. vulgata*, and typically favours 'wetter' conditions in the littoral zone found on shallow gradient rocky shores, also home to encrusting coralline algae (Firth and Crowe 2010). Shore slope as an important modifier of desiccation may allow greater persistence of macroalgae on more horizontal surfaces, and may mediate foraging activities of important grazers, such as patellid limpets (Benedetti-Cecchi et al. 2000).

Similarly, the importance of complexity in explaining abundance differences between sites may not be entirely due to exposure. Greater substrate complexity tends to dissipate wave energy, where shoaling and substrate porosity increase bottom friction (Mork 1996, Ferrario et al. 2014). However, increased substrate heterogeneity may complicate the interaction with hydrodynamic forces and the benthic community leading to microhabitats of greater exposure and relative shelter (Folley et al. 2010). Furthermore, substrate complexity may provide escape from several important ecological stressors, including desiccation, predation, and changes in temperature and salinity, as well as creating additional surface area for organisms to exploit (Johnson et al. 2003).

## Conclusions

Wave energy extraction may play some role in ameliorating the ecological consequences of climate-induced changes in wave height, at least at the scale of local device deployment. Although recent aspirations of the development of the WEC industry have not been realised, the comprehensive rocky shore survey and research described here is providing evidence well placed to inform the offshore renewable energy industry as it moves towards industrial-scale deployments of devices (Simec Atlantis 2022) and marine ecosystems are coming under increasing threat from climatic changes and other anthropogenic developments (Frost et al. 2016). With increasing pressure from multiple users of the marine resource and global changes in climate affecting marine communities, the effects of changes in wave exposure on species distribution will become increasingly important (Blanchette et al. 2008), particularly so at smaller spatial scales. Changes in temperature remain most likely to drive shifts in distributions at geographical scales.

In this study, detectable shifts in abundance of key structuring species on exposed rocky shores on WMO are predicted following changes in wave height consequent on energy extraction and climatic change. Ecological responses are expected to be highly site specific where a given species may exhibit contrasting changes in abundance at locations in relatively close proximity to one another. There is evidence that the role of topographic variables on rocky shore communi-

ties may be specific to individual community members. In short, exposure may mean different things to different receptor species.

## Acknowledgements

The authors wish to thank the following organizations and individuals: Lucy Bricheno and Judith Wolf of the National Oceanographic Centre, Liverpool, for providing wave scaling data based on their models, and the Marine Alliance of Science and Technology in Scotland for support through their Writing Retreats. Thanks also to the anonymous reviewers who have taken the time to provide critical input which has improved this manuscript.

## Author contributions

Conceptualization: A.W., J.S., and M.C.B.; data curation: A.W., S.W., and M.C.B.; formal analysis: A.W., S.W., and M.C.B.; funding acquisition: A.W. and J.S.; investigation: A.W. and S.W.; methodology: all authors; project administration: A.W.; resources: J.S. and V.V.; software: M.C.B. and S.W.; supervision: J.S., V.V., and M.C.B.; validation: A.W., S.W., and M.C.B.; visualization: A.W., S.W., and M.C.B.; writing - original draft: A.W., S.W., and M.C.B.; writing - review & editing: all authors.

*Conflict of interest:* All the authors declare that they have no conflicts of interest.

## Funding

This work was supported by the Engineering and Physical Sciences Research Council (EPSRC) SuperGen II PhD Studentship and the EPSRC EcoWatt 2050 programme (EPSRC Grand Challenge II Grant Ref: EP/K012851/1);

## Data availability

The data underlying this article will be shared on reasonable request to the corresponding author.

## Appendix 1: Abundance scales used for intertidal organisms, after Crisp and Southward (1958) modified by Hiscock (1981). S: super abundant; A: abundant; C: common; F: frequent; O: occasional; R: rare. Organisms not seen during a 45-minute site visit despite searching were recorded as N: absent.

### Barnacles

S: 300–499 per 0.01 m<sup>2</sup>, 3–4 cm<sup>-2</sup>  
 A: 100–299 per 0.01 m<sup>2</sup>, 1–2 cm<sup>-2</sup>  
 C: 10–99 0.01 m<sup>-2</sup>  
 F: 1–9 per 0.01 m<sup>2</sup>  
 O: 1–99 m<sup>-2</sup>  
 R: <1 m<sup>-2</sup>

### *Patella* spp. ≥ 10 mm,

*Littorinalittorea* (juveniles and adults),  
*L.mariae/obtusata*(adults)  
 S: 10–19 per 0.1 m<sup>2</sup>  
 A: 5–9 per 0.1 m<sup>2</sup>  
 C: 1–4 per 0.1 m<sup>2</sup>

F: 5–9 m–2

O: 1–4 m–2

R: <1 m–2

*Littorina* “*saxatilis*,”

*Patella* <10 mm, *L.mariae/obtusata*juv.

S: 20–49 per 0.1 m<sup>2</sup>

A: 10–19 per 0.1 m<sup>2</sup>

C: 5–9 per 0.1 m<sup>2</sup>

F: 1–4 per 0.1 m<sup>2</sup>

O: 1–9 m–2

R: <1 m–2

*Nucella lapillus* (>3 mm), *Gibbula* spp.

S: 5–9 0.1 m–2

A: 1–4 0.1 m–2

C: 5–9 m–2, sometimes more

F: 1–4 m–2, locally sometimes more

O: <1 m–2, locally sometimes more

R: Always < 1 m–2

*Mytilusedulis*

S: 50%–79% cover

A: 20%–49% cover

C: 5%–19% cover

F: Small patches, 5%; ≥10 small ind. per 0.1 m<sup>2</sup>; ≥1 large ind. per 0.1 m<sup>2</sup>

O: 1–9 small ind. per 0.1 m<sup>2</sup>; 1–9 large ind. m–2; no patches except small ind. in crevices

R: <1 m–2

*Pomatoceros* sp.

A: ≥50 tubes per 0.01 m<sup>2</sup>

C: 1–49 tubes per 0.01 m<sup>2</sup>

F: 1–9 tubes per 0.1 m<sup>2</sup>

O: 1–9 tubes m<sup>2</sup>

R: <1 tube m–2

*Spirorbiniidae*

A: ≥5 cm–2 on appropriate substrata; >100 per 0.01 m<sup>2</sup> generally

C: Patches of ≥ 5 cm–2; 1–100 per 0.1 m<sup>2</sup> generally

F: Widely scattered small groups; 1–9 per 0.1 m<sup>2</sup> generally

O: Widely scattered small groups; <1 per 0.1 m<sup>2</sup> generally

R: <1 m–1

**Sponges, hydroids, bryozoa**

A: Present on ≥ 20% of suitable surfaces

C: Present on 5%–19% of suitable surfaces

F: Scattered patches; <5% cover

O: Small patch or single sprig in 0.1 m<sup>2</sup>

R: <1 patch over strip; 1 small patch or sprig per 0.1 m<sup>2</sup>

**Lichens, lithothamnia**

S: 50%–79% cover

A: 20%–49% cover

C: 1%–19% cover

F: Large scattered patches

O: Widely scattered patches all small

R: Only 1 or 2 patches

**Algae**

S: 60%–89% cover

A: 30%–59% cover

C: 5%–29% cover

F: <5% cover, zone still apparent

O: Scattered plants, zone indistinct

R: Only 1 or 2 plants

## Appendix 2: Species list used for abundance recording in this study.

### Crustacea

*Chthamalus montagui*

*Chthamalus stellatus*

*Semibalanus balanoides*

### Mollusca

*Calliostoma zizyphinum*

*Gibbula cineraria*

*Gibbula umbilicalis*

*Littorinidae*

*Mytilus edulis*

*Nucella lapillus*

*Patella ulyssiponensis*

*Patella vulgata*

*Tectura testudinalis*

### Cnidaria

*Actinia equina*

*Urticina felina*

### Porifera

*Halichondria panicea*

### Chlorophyta

*Cladophora* sp.

*Ulva intestinalis*

*Ulva lactuca*

### Rhodophyta

*Callithamnion* sp.

*Ceramium* sp.

*Chondrus crispus*

*Corallina officinalis*

*Dumontia cortorta*

*Lomentaria articulata*

*Mastocarpus stellatus*

*Osmundea hybrida*

*Osmundea pinnatifida*

*Palmaria palmata*

*Polysiphonia* sp.

*Porphyra umbilicalis*

### Phaeophyceae

*Alaria esculenta*

*Ascophyllum nodosum*

*Fucus distichus anceps*

*Fucus serratus*

*Fucus spiralis*

*Fucus spiralis* f. *nanus*

*Fucus vesiculosus*

*Fucus vesiculosus* f. *linearis*

*Halidrys siliquosa*

*Himantalia elongata*

*Laminaria digitata*

*Laminaria hyperborea*

*Leathesia difformis*

*Pelvetia canaliculata*

*Scytosiphon lomentaria*

**Appendix 3: Rocky shore images representative of complexity scores (see Table 1 for details). Top row, left: Bo Skerry, 1; Latha Skerry, 3; Cauldrus, North, 6. Bottom row, left: Upper Barvas, 8; West of Siadar, 10.**

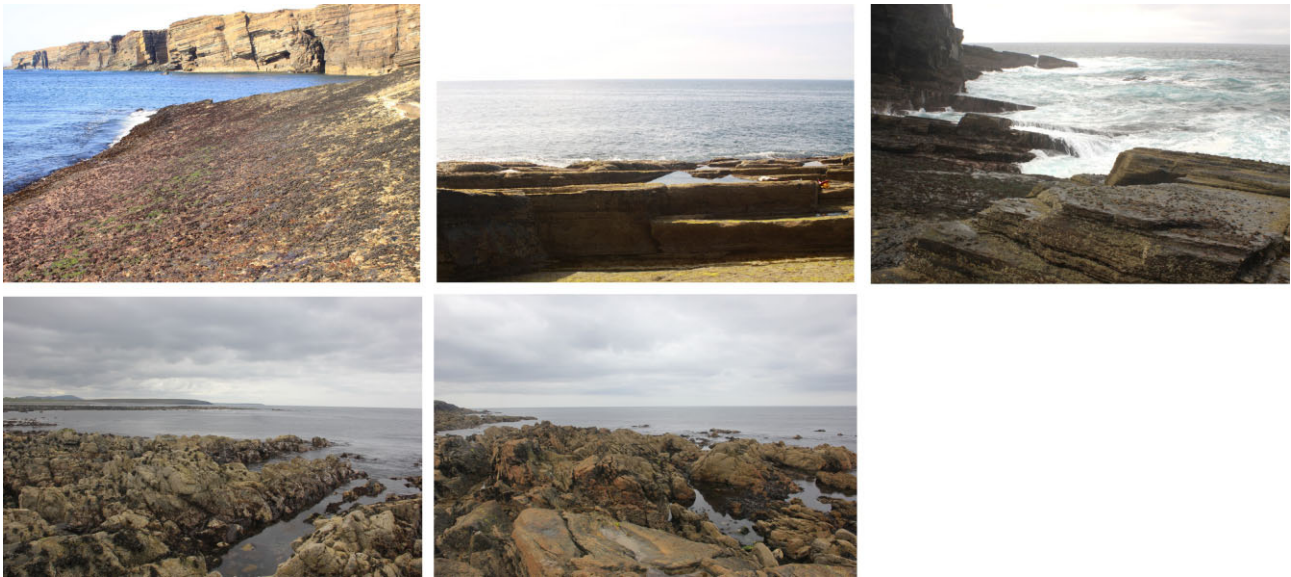


**Figure C1.** Rocky shore images representative of complexity scores (see Table 1 for details). Top row, left: Bo Skerry, 1; Latha Skerry, 3; Cauldrus, North, 6. Bottom row, left: Upper Barvas, 8; West of Siadar, 10.

## Appendix 4: Projected SACFOR scores for select species.

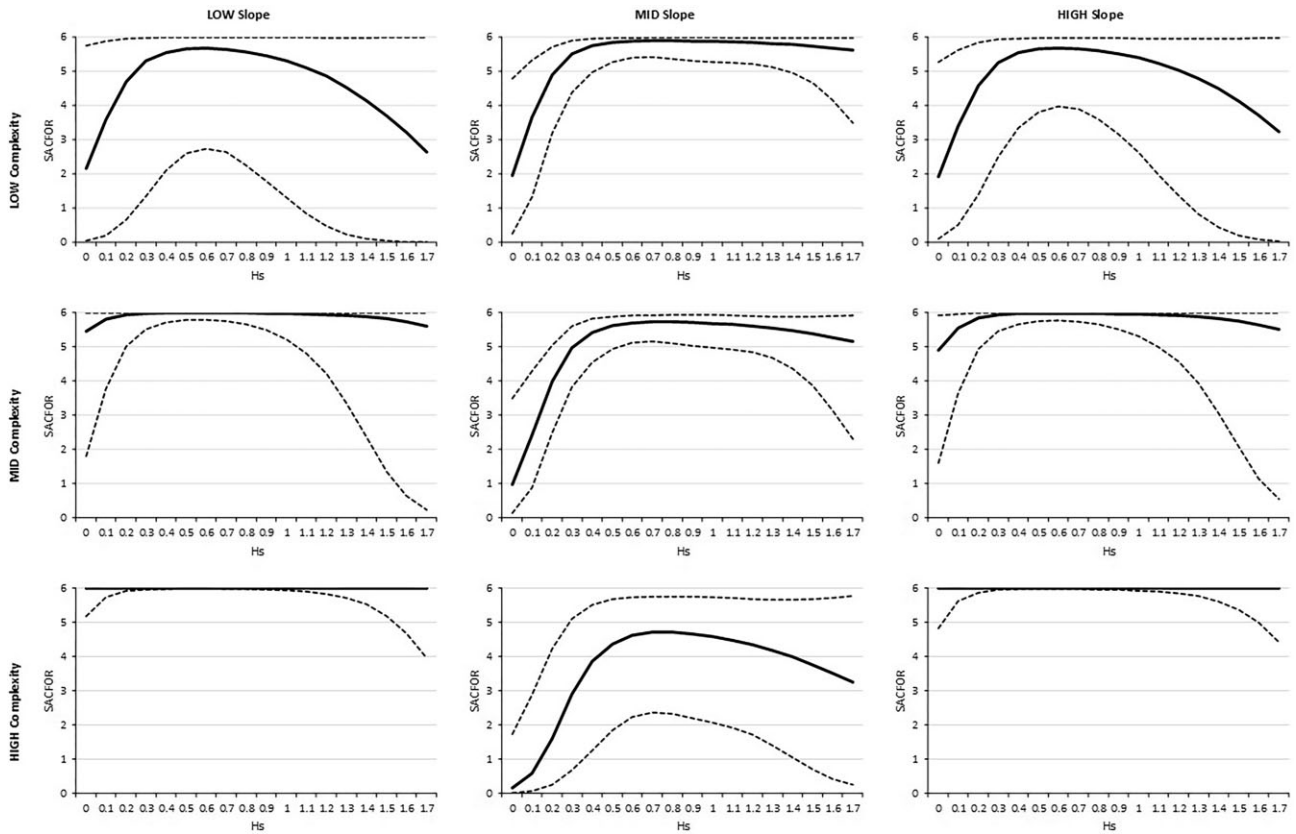


**Figure D1.** Projected SACFOR scores for *Alaria esculenta* in relation to significant wave height at low, mid, and high levels of shore slope and complexity. Bold line is median and broken lines are 2.5 and 97.5 percentiles of the distribution of values from posterior simulation of GAM models.

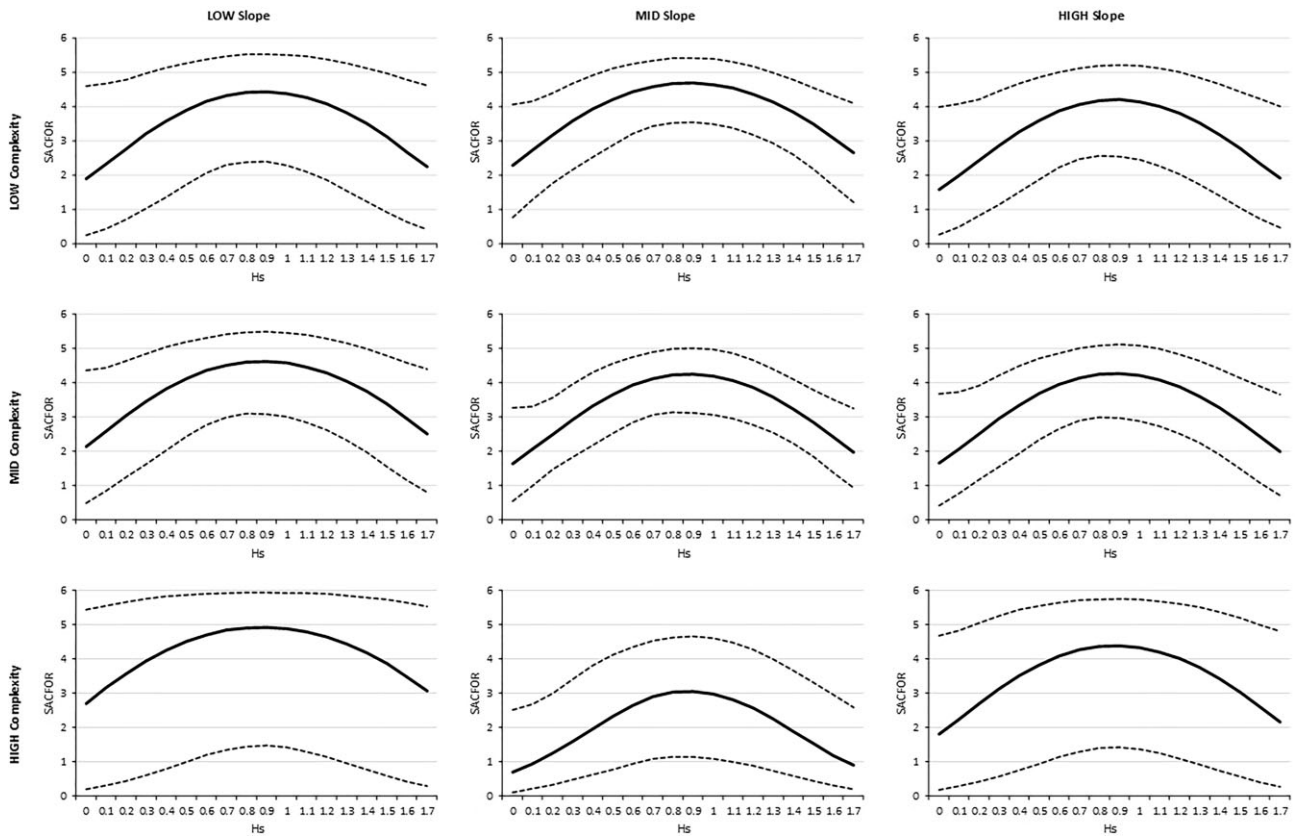


**Figure D2.** Projected SACFOR scores for *Fucus distichus anceps* in relation to significant wave height at low, mid, and high levels of shore slope and complexity. Bold line is median and broken lines are 2.5 and 97.5 percentiles of the distribution of values from posterior simulation of GAM models.

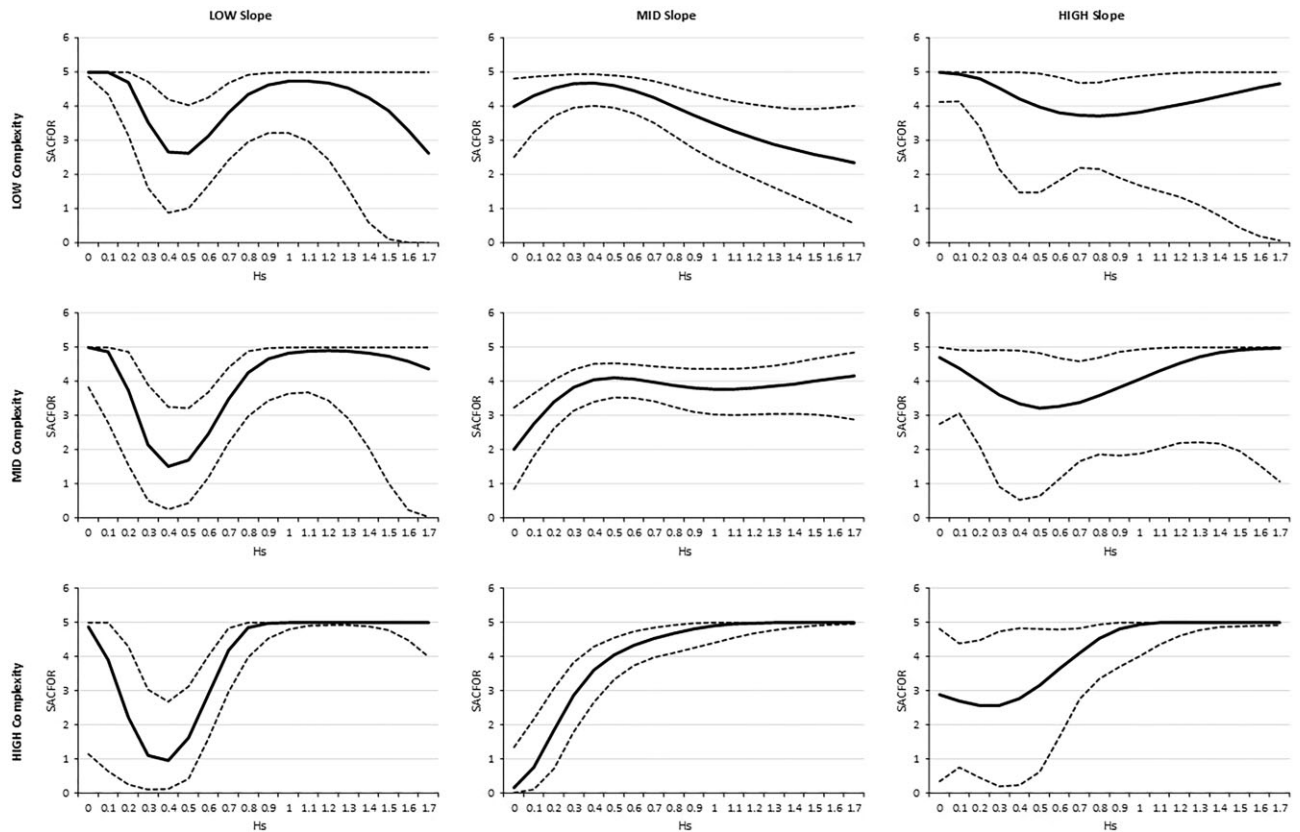


**Figure D3.** Projected SACFOR scores for *Patella ulysiponensis* in relation to significant wave height at low, mid, and high levels of shore slope and complexity. Bold line is median and broken lines are 2.5 and 97.5 percentiles of the distribution of values from posterior simulation of GAM models.

## References

- Ballantine WJ. A biologically defined exposure scale for the comparative description of rocky shores. *Field Stud* 1961;1:1–19.
- Benedetti-Cecchi L, Bulleri F, Cinelli F. The interplay of physical and biological factors in maintaining mid-shore and low-shore assemblages on rocky coasts in the north-west Mediterranean. *Oecologia* 2000;123:406–17. <https://doi.org/10.1007/s004420051028>
- Blanchette CA, O'Donnell MJ, Stewart HL. 2008. Waves as an ecological process. In: *Encyclopedia of Ecology*, 5 (Ed: Jorgensen, Fath). Oxford: Elsevier. 3764–70.
- Bricheno LM, Wolf J. Future wave conditions of Europe, in response to high-end climate change scenarios. *J Geophys Res Oceans* 2018;123:8762–91. <https://doi.org/10.1029/2018JC013866>
- Burel T, Schaal G, Grall J et al. Clear-cut wave height thresholds reveal dominance shifts in assemblage patterns on rocky shores. *Mar Ecol Progr Ser* 2022;683:21–36. <https://doi.org/10.3354/meps13945>
- Burnham KP, Anderson DR. *Model Selection and Multimodel Inference: A Practical Information-Theoretic Approach*, 2nd edn. New York: Springer, 2002, 488.
- Burrows MT, Harvey R, Robb L. Wave exposure indices from digital coastlines and the prediction of rocky shore community structure. *Mar Ecol Progr Ser* 2008;353:1–12. <https://doi.org/10.3354/meps07284>
- Burrows MT, Schoeman DS, Buckley LB et al. The pace of shifting climate in marine and terrestrial ecosystems. *Science* 2011;334:652–5. <https://doi.org/10.1126/science.1210288>
- Cameron L, Doherty R, Henry A et al. Design of the next generation of the Oyster wave energy converter. Third International conference on Ocean Energy, Bilbao. 2010.
- Coe RG, Yu Y-H, Van Rij JA. Survey of WEC Reliability, Survival and Design Practices. *Energies* 2018;11:4. <https://doi.org/10.3390/en11010004>
- Collins M, Knutti R, Arblaster J et al. Long-term climate change: projections, commitments and irreversibility. In: TF Stocker, D Qin, G-K Plattner, M Tignor, SK Allen, J Boschung, A Nauels, Y Xia, V Bex, PM Midgley (eds.). *Climate Change 2013: The Physical Science Basis. Contribution of Working Group I to the Fifth Assessment Report of the Intergovernmental Panel on Climate Change*. Cambridge: Cambridge University Press. 2013.
- Connor DW, Allen JH, Golding N et al. The Marine Habitat Classification for Britain and Ireland Version 04.05. The Marine Habitat Classification for Britain and Ireland Version 15.03. In: *JNCC 2004*. <https://mhc.jncc.gov.uk/resources#version0405> (23 March 2023, date last accessed).
- Copping AE, Hemery LG. *OES-Environmental 2020 State of the Science Report (No. PNNL-29976)*. Richland, WA: Pacific Northwest National Lab. 2020. <https://tethys.pnnl.gov/publications/state-of-the-science-2020> (23 March 2023, date last accessed).
- Crisp DJ, Southward AJ. The distribution of intertidal organisms along the coasts of the English Channel. *J Mar Biol Assoc UK* 1958;37:157–203. <https://doi.org/10.1017/S0025315400014909>
- Crothers JH. Dog-whelks: an introduction to the biology of *Nucella lapillus* (L.). *Field Stud*. 1985;6:291–360.
- Crown Estate. Wave and Tidal (Pentland Firth and Orkney Waters). 2015. <https://www.thecrownestate.co.uk/media/5729/ei-pentland-firth-and-orkneywaters.pdf> (30 September 2022 date last accessed).
- Denny MW. Predicting physical disturbance: mechanistic approaches to the study of survivorship on wave-swept shores. *Ecol Monogr* 1995;65:371–418. <https://doi.org/10.2307/2963496>
- Denny MW. Are there mechanical limits to size in wave-swept organisms? *J Exp Biol* 1999;202:3463–7. <https://doi.org/10.1242/jeb.202.23.3463>
- DHI. *MIKE21 Spectral Wave Model*, 2014 Edition. 2022. <https://www.mikepoweredbydhi.com/>. (23 March 2023, date last accessed).
- ECMWF. 2018. <http://www.ecmwf.int/> (23 March 2023, date last accessed).
- EcoWatt 2050. *EcoWatt 2050 Project Summary*. 2017, 32. <https://www.masts.ac.uk/media/36374/ecowatt2050-booklet.pdf> (23 March 2023, date last accessed).
- EMEC. 2022. <https://www.emec.org.uk/facilities/live-data/wave-data/> (23 March 2023, date last accessed).
- Farcas A, Thompson PM, Merchant ND. Underwater noise modelling for environmental impact assessment. *Environ Impact Assess Rev* 2016;57:114–22. <https://doi.org/10.1016/j.eiar.2015.11.012>
- Ferrario F, Beck MW, Storlazzi C et al. The effectiveness of coral reefs for coastal hazard risk reduction and adaptation. *Nat Commun* 2014;5:3794. <https://doi.org/10.1038/ncomms4794>
- Firth LB, Crowe TP. Competition and habitat suitability: small-scale segregation underpins large-scale coexistence of key species on temperate rocky shores. *Oecologia* 2010;162:163–74. <https://doi.org/10.1007/s00442-009-1441-7>
- Folley M, Elsaesser B, Whittaker TJT. *Analysis of the wave energy resource at the European Marine Energy Centre*. In: *Coasts, Marine Structures and Breakwaters: Adapting to Change*. W. Allsop (ed.). ICE Publishing: London. 2010, 1, 660–9.
- Folley M, Whittaker TJT. Analysis of the nearshore wave energy resource. *Renew Energy* 2009;34:1709–15. <https://doi.org/10.1016/j.renene.2009.01.003>
- Frid C, Androgeni E, Depestele J et al. The environmental interactions of tidal and wave energy generation devices. *Environ Impact Assess Rev* 2012;32:133–9. <https://doi.org/10.1016/j.eiar.2011.06.002>
- Frost M, Bayliss-Brown G, Buckley P et al. A review of climate change and the implementation of marine biodiversity legislation in the United Kingdom. *Aquatic Conserv Mar Freshwater Ecosyst* 2016;26:576–95. <https://doi.org/10.1002/aqc.2628>
- Frost NJ, Burrows MT, Johnson MP et al. Measuring surface complexity in ecological studies. *Limnol Oceanogr Methods* 2005;3:203–10.
- Gaylord B. Biological implications of surf-zone flow complexity. *Limnol Oceanogr* 2000;45:174–88. <https://doi.org/10.4319/lo.2000.45.1.0174>
- Greaves D, Jin S, Richards L et al. Wave energy innovation position paper. *Supergen ORE Hub* 2020;2020, [https://supergen-ore.net/uploads/resources/Wave\\_Energy\\_Innovation\\_-\\_Position\\_Paper.pdf](https://supergen-ore.net/uploads/resources/Wave_Energy_Innovation_-_Position_Paper.pdf) (23 March 2023, date last accessed).
- Hiscock K. The rocky shore ecology of Sullom Voe. *Proc R Soc Edinburgh B Biol Sci* 1981;80:219–40. <https://doi.org/10.1017/S026972700000659X>
- IPCC, Climate change 2014: synthesis report. Contribution of Working Groups I, II and III to the Fifth Assessment Report of the Intergovernmental Panel on Climate Change. IPCC, 2014, 59–60 Geneva, Switzerland.
- Jin S, Greaves D. Wave energy in the UK: Status review and future perspectives. *Renew Sustain Energy Rev* 2021;143:110932. <https://doi.org/10.1016/j.rser.2021.110932>
- Johnson MP, Frost NJ, Mosley MWJ et al. The area-independent effects of habitat complexity on biodiversity vary between regions. *Ecol Lett* 2003;6:126–32. <https://doi.org/10.1046/j.1461-0248.2003.00404.x>
- Johnson MP, Hughes RN, Burrows MT et al. Beyond the predation halo: small scale gradients in barnacle populations affected by the refuge value of crevices. *J Exp Mar Biol Ecol* 1998;231:163–70. [https://doi.org/10.1016/S0022-0981\(98\)00055-0](https://doi.org/10.1016/S0022-0981(98)00055-0)
- Langhamer O. The location of offshore wave power devices structures epifaunal assemblages. *International Journal of Marine Energy* 2016;16:174–80. <https://doi.org/10.1016/j.ijome.2016.07.007>
- Lewis JR. *The Ecology of Rocky Shores*. London: Hodder & Stoughton. 1964.
- Lindeboom HJ, Kouwenhoven HJ, Bergman MJN et al. Short-term ecological effects of an offshore wind farm in the Dutch coastal zone; a compilation. *Environ Res Lett* 2011;6:035101. <https://doi.org/10.1088/1748-9326/6/3/035101>
- Lohse DP, Gaddam RN, Raimondi PT. Predicted effects of wave energy conversion on communities in the nearshore environment.

- In: *Developing Wave Energy In Coastal California: Potential Socio-Economic And Environmental Effects*, California Energy Commission. Sacramento; 2008.
- Lowe RJ, Falter JL, Koseff JR *et al.* Spectral wave flow attenuation within submerged canopies: Implications for wave energy dissipation. *J Geophys Res Oceans* 2007;112:C5–18. <https://doi.org/10.1029/2006JC003605>
- Marine Scotland. 2022. <https://marine.gov.scot/maps/1061> (23 March 2023, date last accessed).
- Mieszowska N, Kendall MA, Hawkins SJ *et al.* Changes in the range of some common rocky shore species in Britain—a response to climate change? *Hydrobiologia* 2006;555:241–51. <https://doi.org/10.1007/s10750-005-1120-6>
- Mork M. The effect of kelp in wave damping. *Sarsia* 1996;80:323–7. <https://doi.org/10.1080/00364827.1996.10413607>
- Munda IM. The structure and distribution of Fucacean associations in the Icelandic coastal area. *Acta Botanica Islandica* 2004;14:103–59.
- Neill SP, Vögler A, Goward-Brown AJ *et al.* The wave and tidal resource of Scotland. *Renew Energy* 2017;114:3–17. <https://doi.org/10.1016/j.renene.2017.03.027>
- O'Hara Murray RB, Gallego A. Data review and the development of realistic tidal and wave energy scenarios for numerical modelling of Orkney Islands waters. *Ocean Coast Manage* 2017;147:6–20. doi:10.1016/j.ocecoaman.2017.03.011
- Parmesan C, Yohe G. A globally coherent fingerprint of climate change impacts across natural systems. *Nature* 2003;421:37–42. <https://doi.org/10.1038/nature01286>
- Peregrine DH. Breaking waves on beaches. *Annu Rev Fluid Mech* 1983;15:149–78. <https://doi.org/10.1146/annurev.fl.15.010183.001053>
- Powell HT. New records of *Fucus distichus* subspecies for the Shetland and Orkney Islands. *British Phycol Bull* 1963;2:247–54. <https://doi.org/10.1080/00071616300650091>
- R Core Team. *R: A language and environment for statistical computing*. Vienna: R Foundation for Statistical Computing. 2018.
- Riahi K, Rao S, Krey V *et al.* RCP 8.5—A scenario of comparatively high greenhouse gas emissions. *Clim Change* 2011;109:33. <https://doi.org/10.1007/s10584-011-0149-y>
- Ruuskanen A, Back S, Reitalu T. A comparison of two cartographic exposure methods using *Fucus vesiculosus* as an indicator. *Mar Biol*, 1999;134:139–45 <https://doi.org/10.1007/s002270050532>
- Ruuskanen AT, Nappu NP Morphological differences in *Fucus gardneri* between two shores with equal cartographic exposure values but different levels of wave action. *Annales Botanici Fennici* 2005;42:27–33.
- Scottish Government. *Pilot Pentland Firth and Orkney Waters Marine Spatial Plan*. Scottish Government. 2016, 228. <https://www.gov.scot/publications/pilot-pentland-firth-orkney-waters-marine-spatial-plan/documents/> (23 March 2023, date last accessed).
- Shields MA, Woolf DK, Grist EPM *et al.* Marine renewable energy: the ecological implications of altering the hydrodynamics of the marine environment. *Ocean Coast Manage* 2011;54:2–9. <https://doi.org/10.1016/j.ocecoaman.2010.10.036>
- Siddon CM, Witman JD. Influence of chronic, low-level hydrodynamic forces on subtidal community structure. *Marine Ecology Progress Series* 2003;261:99–110. <https://doi.org/10.3354/meps261099>
- Simec A. 2022. <https://simecatlantis.com/tidal-stream/meygen/> (23 March 2023, date last accessed).
- Smith JM. Surf Zone Hydrodynamics. In: Z. Demirbilek (ed.), *Coastal Engineering Manual, Part II, Coastal Hydrodynamics, Chapter II-4, Engineer Manual 1110-2-1100*. Washington, DC: U.S. Army Corps of Engineers. 2003.
- Sundblad G, Bekkby T, Isæus M *et al.* Comparing the ecological relevance of four wave exposure models. *Estuarine Coastal Shelf Sci* 2014;140:7–13. <https://doi.org/10.1016/j.ecss.2014.01.008>
- Tay ZY, Venugopal V. Hydrodynamic interactions of oscillating wave surge converters in an array under random sea state. *Ocean Eng* 2017;145:382–94. <https://doi.org/10.1016/j.oceaneng.2017.09.012>
- Thomas MLH A physically derived exposure index for marine shorelines. *Ophelia*, 1986;25:1–13. <https://doi.org/10.1080/00785326.1986.10429719>
- Vadas RL, Wright WA, Miller SL. Recruitment of *Ascophyllum nodosum*: wave action as a source of mortality. *Marine Ecology Progress Series* 1990;61:263–72. <https://doi.org/10.3354/meps061263>
- Venugopal V, Nimalidinne R Wave resource assessment for Scottish waters using a large scale North Atlantic spectral wave model. *Renewable Energy* 2015;76:503–25. [10.1016/j.renene.2014.11.056](https://doi.org/10.1016/j.renene.2014.11.056)
- Venugopal V, Nimalidinne R, Vögler A Numerical modelling of wave energy resources and assessment of wave energy extraction by large scale wave farms. *Ocean Coast Manage* 2017;147:37–48. [10.1016/j.ocecoaman.2017.03.012](https://doi.org/10.1016/j.ocecoaman.2017.03.012)
- Waggitt JJ, Cazenave PW, Torres R *et al.* Predictable hydrodynamic conditions explain temporal variations in the density of benthic foraging seabirds in a tidal stream environment. *ICES J Mar Sci Journal du Conseil* 2016;73:2677–86. <https://doi.org/10.1093/icesjms/fsw100>
- WAMIT. Wave interaction modelling tool. 2022. <https://www.wamit.com/> (23 March 2023, date last accessed).
- Want A *Detecting responses of rocky shore organisms to environmental change following wave energy extraction*. Unpublished PhD Thesis, Heriot-Watt University. 2017. <https://www.ros.hw.ac.uk/handle/10399/3284> (23 March 2023, date last accessed).
- Want A, Beharie RA, Bell MC *et al.* Baselines and monitoring methods for detecting impacts of hydrodynamic energy extraction on intertidal communities of rocky shores. In: *Marine Renewable Energy Technology and Environmental Interactions*. Netherlands: Springer. 2014, 21–38.
- Wave Energy Roadmap 2020 for the UK. 2020. [https://supergen-ore.net/uploads/resources/Wave\\_Energy\\_Road\\_Map\\_-\\_Realising\\_the\\_potential\\_of\\_Wave\\_Energy\\_in\\_the\\_next\\_10\\_to\\_15\\_years.pdf](https://supergen-ore.net/uploads/resources/Wave_Energy_Road_Map_-_Realising_the_potential_of_Wave_Energy_in_the_next_10_to_15_years.pdf) (23 March 2023, date last accessed).
- Wilding TA, Palmer EJJ, Polunin NVC. Comparison of three methods for quantifying topographic complexity on rocky shores. *Mar Environ Res* 2010;69:143–51. <https://doi.org/10.1016/j.marenvres.2009.09.005>
- Wilhelmsson D, Malm T. Fouling assemblages on offshore wind power plants and adjacent substrata. *Estuarine Coastal Shelf Sci* 2008;79:459–66. <https://doi.org/10.1016/j.ecss.2008.04.020>
- Wilson B, Batty RS, Daunt F *et al.* Collision risks between marine renewable energy devices and mammals, fish and diving birds: report to the Scottish Executive. 2006.
- Wolcott B. Mechanical size limitation and life-history strategy of an intertidal seaweed. *Mar Ecol Progr Ser* 2007;338:1–10. <https://doi.org/10.3354/meps338001>
- Wood S, Pya N, Säfken B. Smoothing parameter and model selection for general smooth models. *J Am Statist Assoc*, 2016;111:1548–63. <https://doi.org/10.1080/01621459.2016.1180986>
- Wood SN. *Generalized Additive Models. An Introduction with R. Second Edition*. Boca Raton: Chapman & Hall/CRC, 2017, 476.
- Woolf DW, Wolf J. Impacts of climate change on storms and waves. *MCCIP Science Review* 2013;2013:20–6.
- Yemm R, Pizer D, Retzler C *et al.* Pelamis: experience from concept to connection. *Philos Trans R Soc A* 2012;370:365–80. <https://doi.org/10.1098/rsta.2011.0312>

Handling Editor: Steven Degraer